



AIAA SciTech 2015 Kissimmee, Fl, USA  
 Fluid Dynamics: RANS/LES Modeling and Applications

# Use of Symbolic Regression for construction of Reynolds-stress damping functions for Hybrid RANS/LES

Jack Weatheritt\* and Richard D. Sandberg†

*Faculty of Engineering and the Environment, University of Southampton, Southampton, SO17 1BJ, UK*

A novel approach to turbulence model development is applied to formulate a Hybrid RANS/LES methodology suitable on coarse meshes. The Reynolds-stress damping function in the Flow Simulation Methodology (FSM) framework is difficult to formulate rigorously from first principles, however it is critical to the success of the model. The damping function dictates locally and instantaneously the contribution level of a RANS model required to supplement structures resolved by the grid. The current formulation is a damping of the turbulent length scale in a nonlinear explicit algebraic stress RANS closure. This turns the eddy viscosity into a sub-grid scale model. In this proposal Symbolic Regression, an evolutionary process according to survival of the fittest, is used to build a new damping function. A population of randomly generated damping functions is evolved by measuring how closely they represent an idealized form. This ideal dataset is generated by filtering DNS to represent a pseudo FSM flow field. In the present study DNS of a turbulent pipe flow is used. Hybrid RANS/LES using the new damping function is performed on two different test cases. Results are presented on coarse meshes for two dimensional periodic hills and inline tandem cylinders, for which the modified FSM performs very well.

## Nomenclature

FSM	Flow Simulation Methodology
RANS	Reynolds-Averaged Navier-Stokes' Equations
SGS	Sub-grid scale
(V)LES	(Very) Large Eddy Simulation
DES	Detached Eddy Simulation
EASM	Explicit Algebraic Stress Model
SST	Menter Shear Stress Transport RANS model
SSG	Speziale, Sarkar and Gatski EASM RANS model

$\Delta$	Grid width
$F$	Contribution (Damping) function
$k$	Turbulent kinetic energy
$\varepsilon$	Turbulent kinetic energy dissipation rate
$\ell_k$	Kolmogorov length scale
$\ell_{RANS}$	RANS integral length scale
$T$	Transfer function
$\tau_{ij}$	Turbulence closure
$u_i$	Velocity component
$\nu$	Kinematic viscosity

\*PhD student, Institute for Complex Systems Simulation, jw22g11@soton.ac.uk

†Professor, Aerodynamics and Flight Mechanics Research Group, AIAA senior member

## I. Introduction

The cost of Large Eddy Simulation (LES) is too great for industrially relevant flows, whereas solutions to the Reynolds-Averaged Navier-Stokes (RANS) equations are too inaccurate for many cases. For well resolved LES 80% of the turbulent kinetic energy  $k$  must be resolved.<sup>1</sup> The scales of the remaining energy are smaller than the grid width  $\Delta$  and so must be modeled. Classical sub-grid scale (SGS) models are suitable only when the modeled scales are isotropic. When the SGS model contributes significantly more than 20% of the turbulent kinetic energy, termed Very Large Eddy Simulation (VLES), this constraint is violated and results deteriorate.

Unified Hybrid RANS/LES models have emerged<sup>2,3</sup> and been significantly developed over the last fifteen years as an answer to the cost requirements of LES. In the present literature a plethora of approaches are available.<sup>1,4</sup> Unified models solve the same equations globally, made possible due to the structural similarity of the equations produced by Reynolds-averaging and low-pass filtering the incompressible Navier-Stokes equations,

$$\partial_t \langle u_i \rangle + \langle u_j \rangle \partial_{x_j} \langle u_i \rangle = -\partial_{x_i} \langle p \rangle + \nu \partial_{x_j x_j}^2 \langle u_i \rangle + \partial_{x_j} \tau_{ij}^{MOD}. \quad (1)$$

$\langle u_i \rangle$  is some resolved velocity, depending on the methodology. For RANS  $\langle \cdot \rangle$  is the Reynolds average and  $\tau_{ij}^{MOD} = \tau_{ij}^{RANS}$  is a traditional turbulence model. For LES  $\langle \cdot \rangle$  is a filter and  $\tau_{ij}^{MOD} = \tau_{ij}^{SGS}$  is an SGS model.

Speziale<sup>2</sup> made three postulates that every unified turbulence model should satisfy:

1. The model should reduce to RANS in the coarse grid limit
2. The model should entirely switch off in the fine grid limit (DNS)
3. No explicit filtering or averaging should be applied.

These postulates are especially useful in an industrial context. 1. and 2. reduce, although clearly not alleviate, the importance of mesh generation. Instead a unified model should be sensitive to a given grid by providing the appropriate magnitude of  $\tau_{ij}^{MOD}$ . 3. is primarily to reduce computational costs and remove issues with cells often present in industrial meshes.

The form of Eq. 1 facilitates the conversion of RANS models into unified hybrid RANS/LES methods. The easiest and most popular way to do this is via a length scale damping function,

$$\ell_{HYB} = F(\Delta, \dots) \cdot \ell_{RANS}, \quad (2)$$

in the classical RANS equations. Damping the RANS length scale  $\ell_{RANS}$  increases the destruction of  $k$ , turning it into an SGS quantity.  $F$  is bound between 0 and 1, the former resulting in DNS and the latter resulting in no damping and hence standard RANS is performed.

The success of models of this type depend on the formulation of  $F$ , which largely throughout the literature lacks a rigorous or analytical formulation. Instead  $F$  is formulated on an *ad-hoc* basis depending explicitly or implicitly on the ratio of  $\Delta$  and a turbulent length scale calculable by RANS quantities at runtime.<sup>2,3,5-7</sup> This *ad-hoc* formulation is due to the complexity of the formal derivation induced by the grid filter or any rigid assumptions that must be made.<sup>8</sup>

This paper is motivated by industrial application and so the coarse grid limit is of particular interest. This is deemed to be the most important regime for unified models where major advances in industrial flow prediction are possible. In order for a model to be considered industry friendly, a RANS model must be successfully recovered in this limit. Keeping the postulates of Speziale in mind, a model well calibrated in this regime is more universally applicable than one calibrated for finer meshes. As  $\Delta \rightarrow 0$ , the model contribution to total stress becomes negligible and so the overall error too becomes negligible. However, a model calibrated on a finer mesh does not come with a guarantee for compliance when  $\Delta$  becomes large. In the best case scenario a poorly calibrated URANS model is recovered and in the worst case,  $\tau_{ij}^{MOD}$  does not provide enough dissipation to ensure stability.

Presented here is the application of a more systematic, Big-Data approach to model formulation. Symbolic regression is applied to fit a functional form to an idealized contribution function produced from Filtered DNS (FDNS) data. This methodology has already been applied successfully to finer meshes,<sup>9</sup> but is now extended to look at different FDNS data and an entirely different flow regime. The method is used to ascertain an appropriate functional form and dependence of  $F$  that is sensitive to severely under-resolved

flow fields. There are no modeling assumptions, the only requirement is a list of independent variables you wish the regression analysis to depend on.

The outline of this paper is as follows. The hybrid framework used throughout this paper is presented in Section II. The regression analysis is presented in Section III. Section IV looks at the application of the new damping function to coarse meshes for the classical periodic hills test case<sup>10</sup> and also for the more challenging inline tandem cylinders.<sup>11</sup> Finally, Section V looks at the future of this work.

## II. The FSM Framework

The hybrid framework chosen is the latest formulation of Flow Simulation Methodology (FSM) of Weinmann *et al.*<sup>12</sup> although the symbolic regression method is not restricted to this approach and the results from the process are easily implemented in another framework. The FSM damping function is defined as

$$F = \min \left( F^{FSM}(\Delta, \ell_k, \ell_{RANS}) \cdot F^{SHIELD}, 1 \right), \quad (3)$$

where the shielding function  $F^{SHIELD}$  forces the near wall switch to RANS mode before the buffer layer. This alleviates grid induced separation and reduces  $\Delta_x$  and  $\Delta_z$  requirements for resolving structures in the boundary layer.  $F^{SHIELD}$  is defined as,

$$F^{SHIELD} = \frac{1}{1 - f_b}, \quad (4)$$

where  $f_b$  is from the Menter<sup>13</sup>  $k - \omega$ -SST turbulence model designed to be 1 at the wall and 0 in the outer layer. Practically  $f_b$  is limited such that  $f_b < 1$  to avoid a zero denominator in Eq. 4. The functional dependence of  $F^{FSM}$  is on the integral, or RANS, length scale  $\ell_{RANS} = k^{3/2}/\varepsilon$  and the Kolmogorov length scale  $\ell_k = (\nu^3/\varepsilon)^{1/4}$ .

The underlying RANS closure is the nonlinear Explicit Algebraic Stress Model (EASM) of Speziale, Sarkar and Gatski<sup>14</sup> (SSG), chosen for a better redistribution of the anisotropic SGS energy required when  $\Delta$  becomes large. FSM is not restricted to this turbulence model, however current studies show that the SSG closure provides more reliable predictions for a wide range of test cases.

The numerical framework used throughout this paper is OpenFOAM.<sup>15</sup> This allows for an easily manipulated and consistent test bed for FSM alongside other hybrid closures. OpenFOAM however is an unstructured code and this limits the definition of  $\Delta$ . Currently simulations in this paper have been performed using the cube root volume, but it is noted that the impact of different definitions of  $\Delta$  should be studied.

The numerical scheme adopted is the hybrid central/upwinding scheme of Weinmann *et al.*<sup>12</sup> This allows for central differencing in LES regions and upwinding in RANS regions.

## III. Construction of the Damping Function

The functional form of the contribution function is found from an idealized dataset via a refined regression analysis. Hybrid RANS/LES is mimicked by a coarse filtering of a DNS (FDNS) flow field. The scales that are removed by the filter represent the sub-grid scales that should be modeled by  $\tau_{ij}^{MOD}$ . The scales not removed by the filter are those that should be resolved in a hybrid RANS/LES simulation.  $\Delta$  is related to the filter's transfer function  $T$ , assuming the test filter will remove wavelengths smaller than  $\kappa_c$  where  $T(\kappa_c) = 0.5$ .

The ideal form of the contribution function describes the amount of resolved stress over total stress, as derived by Germano,<sup>16</sup>

$$F = 1 - \frac{\tau_{ij}^{RANS} \tau_{ij}^{RES}}{\tau_{mn}^{RANS} \tau_{mn}^{RANS}}, \quad (5)$$

where  $\tau_{ij}^{RES} = \langle u_i u_j \rangle - \langle u_i \rangle \langle u_j \rangle$  is the time averaged resolved stress. Due to this time average, Eq. (5) is not suitable for actual FSM — but can be calculated for FDNS data.

Figure 1 shows this function for well resolved in house DNS turbulent pipe data at Re=3350 based on radius  $r$  with a 2<sup>nd</sup> order explicit test filter applied. Temporal averaging over 101 snapshots and spatial averaging across the homogeneous directions were used in the calculation of Eq. (5). Convergence in the bulk

flow was not achieved due to the longer eddy turnover time, however this is not deemed an issue because the independent variables are affected in the same way, so smooth functions are still produced.

The original FSM damping function,<sup>2</sup>

$$F_{SPEZIALE} = 1 - \exp\left(-\beta \frac{\Delta}{\ell_k}\right), \quad (6)$$

where  $\beta = 0.001$  is also plotted in Fig 1. This function was calibrated for the DNS limit and it is shown that as  $\Delta \gg \ell_k$ , the function fails to provide the correct damping.

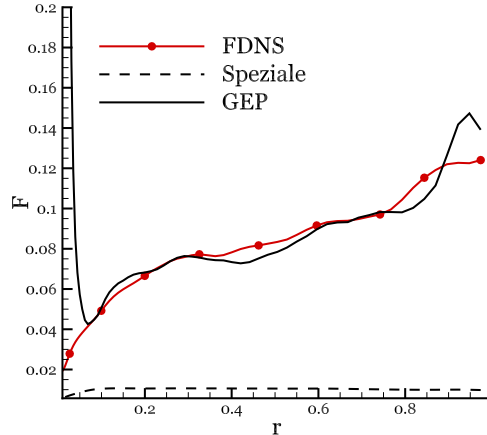


Figure 1: Comparison of Contribution Functions

Symbolic Regression is used to find a functional form that better describes the FDNS data. The evolutionary framework selected for this process is Gene Expression Programming<sup>17</sup> (GEP) because of its suitability for regression problems.  $F = F(\Delta/\ell_k, \Delta/\ell_{RANS})$  is assumed. Preliminary tests with the functional form  $F = F(\Delta/\ell_k)$ , as is the case with Eq. (6), found no satisfactory solutions, indicating that  $\Delta/\ell_k$  is a poor indicator for damping on coarse meshes.

An initial population of random functions, generated from the independent variables  $\Delta/\ell_k, \Delta/\ell_{RANS}$ , random constants and the operators  $+, -, \times, /, \log, \exp$  is evolved according to survival of the fittest — measured by how closely a candidate represents the FDNS data. Should a function be deemed ‘fit’ then it has a high probability of survival and reproducing,<sup>a</sup> otherwise it is likely to die out. A further measure of fitness is added to control the simplicity of solutions. Functions that contain nested operators (i.e.  $\exp(\exp(\exp(\sin(...))))$ ) are severely punished and shorter functions are favored over longer ones.

Figure 1 shows the results from the evolutionary process,

$$F_{GEP} = C_1 \log\left(1 + C_2 \frac{\Delta}{\ell_k}\right)^n \frac{\Delta}{\ell_{RANS}}, \quad (7)$$

where  $C_1, C_2$  and  $n$  are constants.

The evolutionary algorithm is sophisticated enough to find a factor that controls the DNS limit and a factor for controlling the VLES regime. The DNS component,  $\log(1 + C_2 \Delta/\ell_k)^n$ , is now more responsive than Eq. (6) for larger values of  $\Delta/\ell_k$  as required and naturally reduces to zero as  $\Delta \rightarrow 0$ . In practice, this DNS component is individually limited at 1, so as not to interfere with the VLES control. For this simple configuration, the VLES control is linear in  $\Delta/\ell_{RANS}$ , but this needs to be explored for more complex flow fields and different levels of filtering.

Equation (7) closely matches the FDNS contribution function with a discrepancy near the wall. This is because  $\ell_{RANS} \rightarrow 0$  much faster than  $\Delta$  in this region. This is not an issue because Eq. 7 is inserted into Eq. 3, which controls the near wall behavior via the  $F^{SHIELD}$  function.

Finally  $C_i$  and  $n$  are calibrated for a channel flow of friction Reynolds number  $Re_\tau = 550$  with  $N_y = 109$ . The model is calibrated to match  $\langle uv \rangle$ . Whilst correctly reproducing the spectrum from isotropic turbulence is desired and indeed a popular choice for model calibration,<sup>6,18,19</sup> for industrially relevant applications

<sup>a</sup>using parts of a function along with parts of another to form a new population member

correctly predicting the shear stress is vital. A second argument is that for complex geometries, the large structures are going to be highly anisotropic and dictated by large scale motions, whilst the cut off will dictate a large model contribution. Therefore, we believe that isotropic turbulence is not a relevant calibration case for an industrially friendly closure. The constants are found to be  $C_1 = 2.1$ ,  $C_2 = 0.75$  and  $n = 4$ . These constants are fit for coarser meshes. The RANS limit is obtained when  $2.1\Delta = \ell_{RANS}$ . Therefore FSM in this limit successfully recovers the underlying RANS model when no structures can be resolved. The DNS part can then be thought of as a  $C_1$  damping term that lowers this value as  $\Delta \rightarrow 0$ . If a lower bound of 0.65 was placed on  $C_1 \log(1 + C_2 \Delta / \ell_k)^n$  then a Detached Eddy Simulation<sup>19</sup> (DES) methodology (with an alternate near wall treatment) would be recovered. Crucially this alternate formulation is more suitable to coarser grids desirable in industry. To see this last point, consider that for DES the underlying RANS model is not reached until  $\Delta = 1.54\ell_{RANS}$  — which is clearly incorrect and the underlying cause of numerical problems with large grid spacings.

#### IV. Applications

The modified FSM has been applied to two cases — two dimensional periodic hills and inline tandem cylinders.

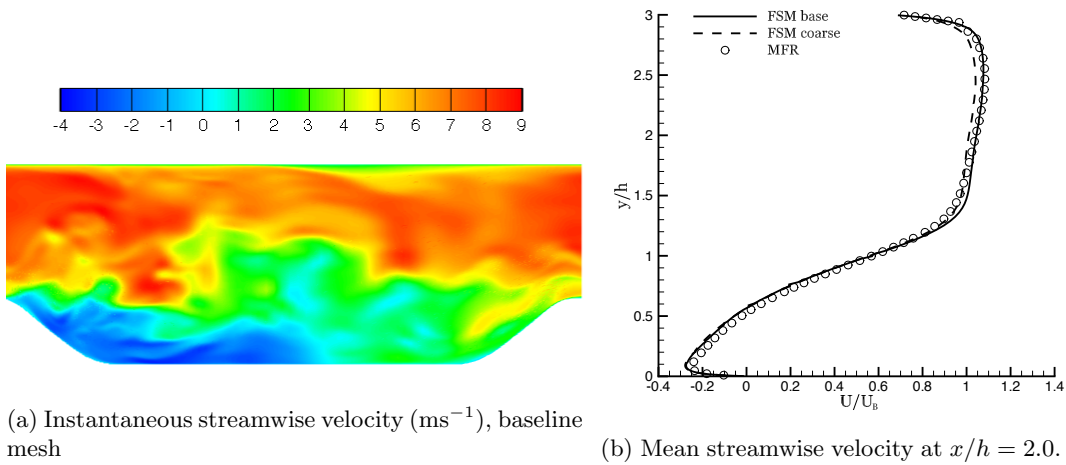


Figure 2: Periodic Hills.

The flow over two dimensional periodic hills at  $Re = 10,595$  based on bulk velocity  $U_b$  and hill height  $h$ , as described in Ref. 10, is a classic hybrid RANS/LES test case. Two grids are used, the first consists of 2,000,000 cells (baseline) and the second 800,000 (coarse). For both meshes, care is taken to ensure proper near wall resolution along the lower surface. The baseline is approximately half the number of points of the reference LES data of Mellen, Fröhlich and Rodi (MFR-LES). Figure 2(a) shows the instantaneous streamwise velocity for the baseline case. One can see the smooth regions near the upper and lower surface where a RANS mode is recovered. Figure 3(a) plots the skin friction coefficient  $C_f$  along the bottom surface, showing good agreement with the reference for both separation and reattachment points. Between the two meshes there is relatively little difference, producing trustworthy results for both resolutions. For both meshes, the magnitude of  $C_f$  is too great in the separation region and results in slightly too long recirculation zones. The baseline case also predicts the commonly observed secondary bubble on the windward side of the hill.

Figure 2(b) and Fig. 3(b) show normal profiles at the streamwise location  $x/H = 2.0$ , corresponding to the downstream base of the hill. This is a particularly challenging region as it crosses the reverse flow and shear layer. The mean streamwise velocity agrees well with the LES data and is reasonably independent of the resolution considered.

The resolution appears to be a sensitive factor for the total turbulent kinetic energy  $k^{TOT}$  and an over prediction is observed for the baseline mesh. Whilst there is some double counting in calculating  $k^{TOT} = k^{RES} + k^{MOD}$ , due to the calibration decision, this is not the whole story. For the baseline mesh, the resolved turbulent kinetic energy is also greater than the reference LES quantity and the near wall RANS layers contain values much too high. After this near wall over prediction, the tangent to the predicted

$k^{TOT}$  on the mesh matches the reference tangential value. It is believed that the shielding function is performing inadequately for this case and alternative formulations could be considered. The coarse mesh provides excellent agreement with the LES  $k^{TOT}$ , which on the one hand is very encouraging and on the other slightly disappointing. For an industrially friendly model, the solution quality should not respond nonlinearly with grid resolution. This is not an uncommon feature of hybrid models, especially for this case. A comprehensive study of DES applied to the periodic hills<sup>20</sup> showed good results, but the agreement was nonlinear in  $\Delta$ . Further a study using the Scale-Adaptive Simulation<sup>21</sup> (SAS) approach showed a similar over prediction of  $k^{TOT}$  for the baseline mesh, implicating a potential underlying issue with the cell topology.

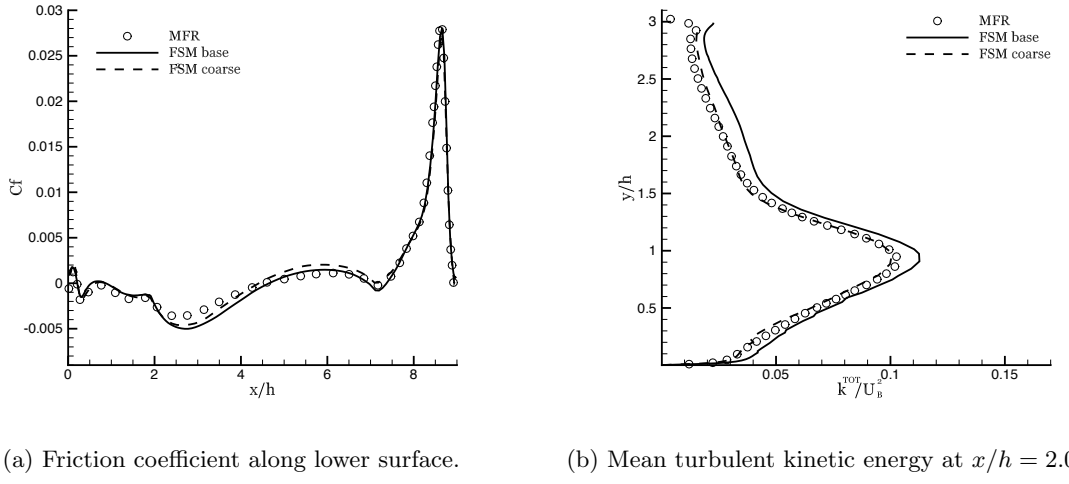
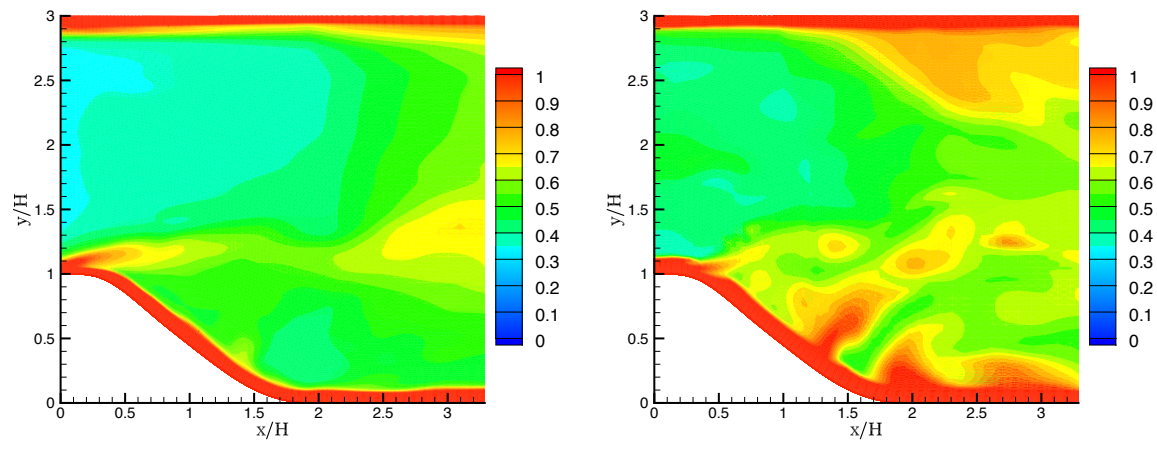


Figure 3: Periodic Hills.

Figure 4 shows the instantaneous values of the contribution function  $F$ . The shear-layer is pronounced due to the increased amount of modeling required there. On the coarse mesh, the contribution function can clearly be seen to adapt to the required level of modeling demanded by the larger  $\Delta$ . Near the boundaries the RANS mode is completely recovered, which is therefore responsible for modeling the unsteady separation point.



(a) Baseline mesh.  
(b) Coarse mesh.  
Figure 4: Periodic Hills: instantaneous values of the damping function  $F$ .

Inline tandem cylinders present a significant modeling challenge to correctly calculate the shear layer roll-up and the upstream wake interaction with the second cylinder surface. The setup is fully described in Ref. 11

and is schematically shown in Fig. 5. The mesh consists of just 1,000,000 cells, which is approximately 7 times cheaper than the next cheapest hybrid methodology submitted to the BANC workshop<sup>11</sup> without significant deterioration of results. To highlight the challenge of this mesh, a variety of other hybrid methodologies were tested and none even gave a physical representation of the flow field. This includes delayed DES,<sup>22</sup> which cannot reproduce the RANS limit as alluded to in Section III, resulting in numerical oscillations polluting the flow field. FSM with Eq. 6 was numerically unstable and SAS<sup>21</sup> failed to predict the turbulence in the wake of the first cylinder, severely compromising first order statistics around the downstream cylinder.

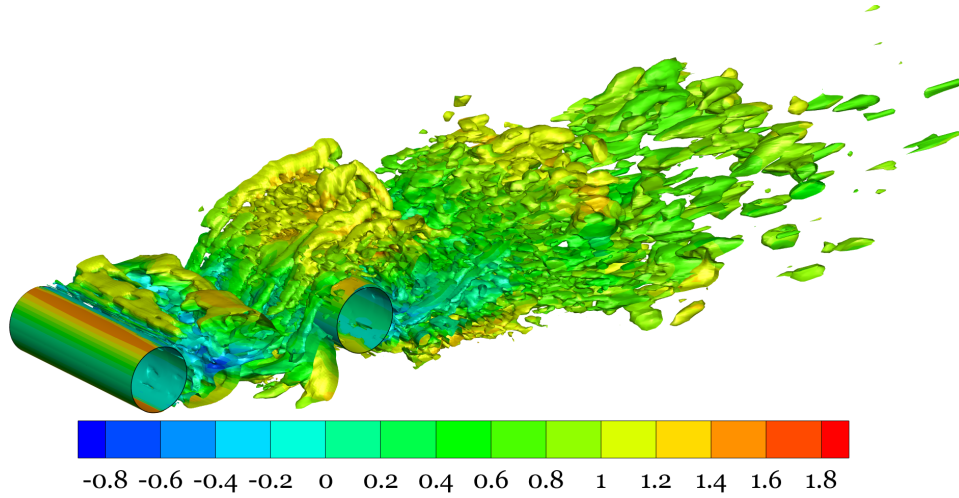


Figure 5: Tandem Cylinders: Instantaneous Q-criterion isosurfaces for the FSM at  $1.7 \times 10^5 \text{ s}^{-2}$  colored by streamwise velocity  $U/U_0$ .

Results are compared against experimental data from the NASA Langley Research Center<sup>23</sup> in Figs. 6(a,b) and 7(a). The steady pressure coefficients are well predicted upstream and downstream, with a deviation in the peaks on the downstream cylinder. This is likely down to a loss of energy in the wake of the first cylinder and the less negative value at the peaks is likely to result in a slightly early separation. The peaks for the upstream cylinder  $C_p$  rms are associated with the separation around this cylinder and the FSM flow field correctly matches the location of greatest fluctuation. There is however an over prediction of the overall magnitude. The downstream rms values are particularly encouraging, which implies that the correct wake-body interaction has been predicted.

The velocity magnitude in between the cylinders is in good agreement with the reverse flow region but starts to deteriorate towards the second cylinder, indicating too much energy is being drained by the shed vortices.

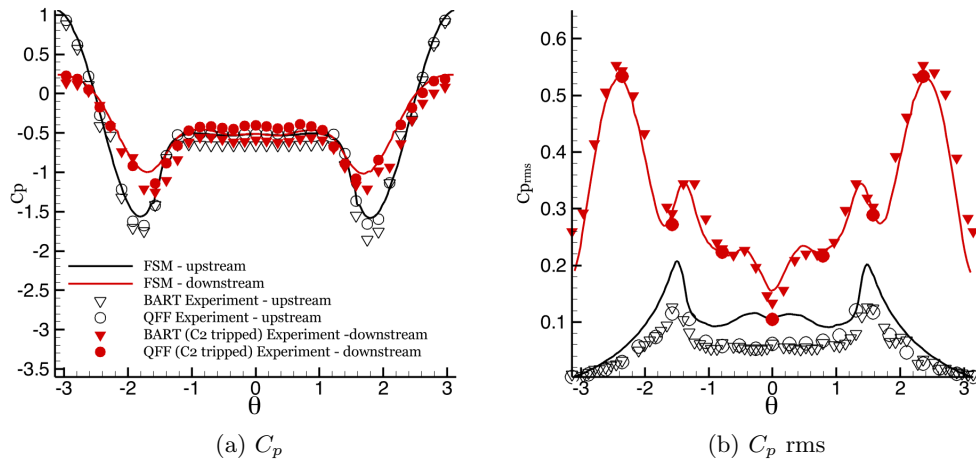


Figure 6: Tandem Cylinders.

Figure 5 is a plot of instantaneous Q-criterion. The varying size of the resolved structures along the flow field is a result of the FSM adapting locally to the available grid resolution and turbulence present. Figure 7(b) shows that  $\Delta$  reaches 300 times the Kolmogorov limit in the shed vortices, which highlights the coarse nature of this simulation.

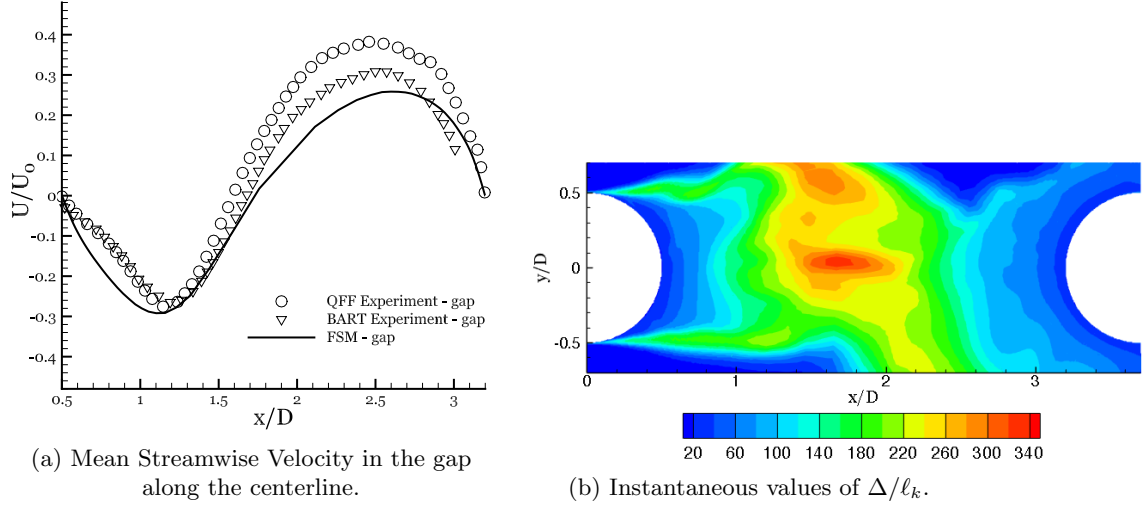


Figure 7: Tandem Cylinders.

Figure 8 is a contour plot of instantaneous values of  $F$  between the two cylinders at mid-span. The range of  $F$  is pronounced — outside of the wake and vortices the model reverts entirely to RANS but is able to quickly switch to VLES in the presence of turbulence. The contribution function adapts further in this region also, the level of modeling is at its lowest in the shed vortex-second cylinder interaction and reaches moderate levels between the reverse flow behind the upstream cylinder and the shed vortex.

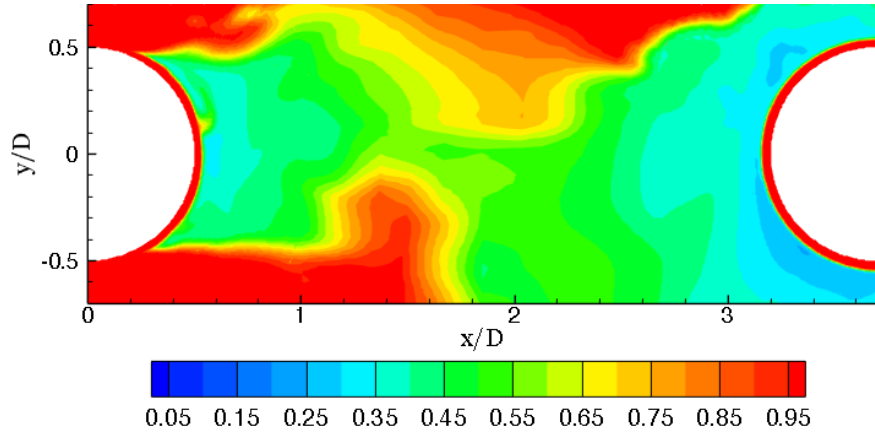


Figure 8: Tandem Cylinders: Instantaneous values of the damping function  $F$ .

## V. Conclusion and Outlook

A new contribution function  $F$  for FSM has been formulated using a novel technique for turbulence modeling. The function, evolved by survival of the fittest, requires no assumptions about its functional form. Special attention has been paid to making the model industry friendly by ensuring the RANS limit is appropriately recovered. This contribution function has been applied to two different cases. The periodic hills is a moderate saving over LES but the Tandem Cylinders is truly a VLES with far fewer points than other hybrid methodologies applied to the same problem. For both cases the results look promising and capture the flow field well, highlighting the advantage of the new FSM in the RANS limit.

FSM as with most unified models is easy to implement and can be used in conjunction with any RANS

model available in a given code. For this reason the modified FSM should be tested with a variety of RANS closures, in order to test the impact of the model. At the time of writing, the SSG model (used in this paper) is more reliable for a wide range of test cases than other simpler closures, although not necessarily the best performer for a given problem. It is this kind of reliable behavior that is desired and currently there is no reason to change from the SSG.

The methodology for formulating the contribution function can be extended to include more datasets. The next to be considered are the flow fields around a T106A low pressure turbine blade and a turbulent boundary layer. Whilst the latter is expected to confirm a similar functional form to Eq.7 and thus validate the methodology; the separation bubble, free shear-layer and strong pressure gradients produced by the turbine blade geometry should shed new light on the required functional form in more complex flow regions. These datasets can be combined to find a functional form that fits the FDNS data for all three cases.

Further, different level filters can be applied and combined to test the amount of damping required in the fine grid limit simultaneously with the coarse. Performing this analysis should create a model that truly satisfies Speziale's postulates for unified modeling.

## Acknowledgments

Thank you to Patrick Bechlars for making his DNS pipe data available. This work was supported by an EPSRC Doctoral Training Centre grant (EP/G03690X/1).

## References

- <sup>1</sup>Fröhlich, J. and von Terzi, D., "Hybrid LES/RANS Methods for the Simulation of Turbulent Flows," *Progress in Aerospace Sciences*, Vol. 44, 2008, pp. 349–377.
- <sup>2</sup>Speziale, C. G., "Turbulence modeling for time-dependent RANS and VLES: A review," *AIAA Journal*, Vol. 36, No. 2, 1998, pp. 173–184.
- <sup>3</sup>Spalart, P. R., Jou, W.-H., Strelets, M., and Allmaras, S. R., "Comments on the feasibility of LES for wings, and on a Hybrid RANS/LES approach," *Advances in DNS/LES*, edited by C. Liu and Z. Liu, Gayden Press, 1997, pp. 137–147.
- <sup>4</sup>Sagaut, P., Deck, S., and Terracol, M., "Multiscale and multiresolution approaches in turbulence-les, des and hybrid rans/les methods," 2013.
- <sup>5</sup>Kourta, A., "Computation of vortex shedding in solid rocket motors using time-dependent turbulence model," *Journal of propulsion and power*, Vol. 15, No. 3, 1999, pp. 390–400.
- <sup>6</sup>Travin, A., Shur, M., Spalart, P. R., and Strelets, M., "On URANS solutions with LES-like behaviour," *Proc. ECCOMAS*, 2004.
- <sup>7</sup>Girimaji, S. S., "Partially-averaged Navier-Stokes model for turbulence: A Reynolds-averaged Navier-Stokes to direct numerical simulation bridging method," *Journal of Applied Mechanics*, Vol. 73, No. 3, 2006, pp. 413–421.
- <sup>8</sup>Magnier, J. C., *Simulation des grandes échelles (SGE) d'écoulements de fluide quasi incompressibles.*, Ph.D. thesis, Université de Paris Sud., 2001.
- <sup>9</sup>Weatheritt, J. and Sandberg, R. D., "A new Reynolds stress damping function for Hybrid RANS/LES with an evolved functional form," *IUTAM Symposium on Advances in Computation, Modeling and Control of Transitional and Turbulent Flows*, Goa, India, 2014.
- <sup>10</sup>Fröhlich, J., Mellen, C., Rodi, W., Temmerman, L., and Leschziner, M., "Highly resolved large-eddy simulation of separated flow in a channel with streamwise periodic constrictions," *Journal of Fluid Mechanics*, Vol. 526, 2005, pp. 16–66.
- <sup>11</sup>Lockard, D. P., "Summary of the Tandem Cylinder Solutions from the Benchmark problems for Airframe Noise Computations-I Workshop," *AIAA, Aerospace Sciences Meeting Including the New Horizons Forum and Aerospace Exposition*, Orlando, Florida, USA, 2011.
- <sup>12</sup>Weinmann, M., Sandberg, R. D., and Doolan, C., "Tandem cylinder flow and noise predictions using a hybrid RANS/LES approach," *International Journal of Heat and Fluid Flow*, 2014.
- <sup>13</sup>Menter, F. R., "Zonal Two Equation  $k-\omega$  Turbulence Models for Aerodynamic Flows," *AIAA Paper 93-2906*, 1993.
- <sup>14</sup>Speziale, C. G., Sarkar, S., and Gatski, T. B., "Modelling the pressure strain correlation of turbulence: an invariant dynamical systems approach," *Journal of Fluid Mechanics*, Vol. 227, 1991, pp. 245–272.
- <sup>15</sup>"OpenFOAM: The Open Source CFD Toolbox. User Guide." Tech. rep., SGI Corp, 2014.
- <sup>16</sup>Germano, M., "Comment on "Turbulence Modeling for Time-dependent RANS and VLES: A Review"," *AIAA Journal*, Vol. 36, No. 9, 1998.
- <sup>17</sup>Ferreira, C., "Gene Expression Programming: A New Adaptive Algorithm for Solving Problems," *Complex Systems*, Vol. 13, No. 2, 2001, pp. 87–129.
- <sup>18</sup>Shur, M., Spalart, P. R., Strelets, M., and Travin, A., "Detached-eddy simulation of an airfoil at high angle of attack," *Engineering turbulence modelling and experiments*, Vol. 4, 1999, pp. 669–678.
- <sup>19</sup>Strelets, M., *Detached eddy simulation of massively separated flows*, American Institute of Aeronautics & Astronautics, 2001.

<sup>20</sup>Šarić, S., Jakirlić, S., Breuer, M., Jaffrézic, B., Deng, G., Chikhaoui, O., Fröhlich, J., Von Terzi, D., Manhart, M., and Peller, N., "Evaluation of detached eddy simulations for predicting the flow over periodic hills," *ESAIM: proceedings*, Vol. 16, EDP Sciences, 2007, pp. 133–145.

<sup>21</sup>Menter, F. R., Kuntz, M., and Bender, R., "A scale-adaptive simulation model for turbulent flow predictions," *AIAA Paper 2003-0767*, 2003.

<sup>22</sup>Spalart, P. R., Deck, S., Shur, M. L., Squires, K. D., Strelets, M., and Travin, A., "A New Version of Detached-eddy Simulation, Resistant to Ambiguous Grid Densities," *Theoretical and Computational Fluid Dynamics*, Vol. 20, No. 3, 2006, pp. 181–195.

<sup>23</sup>Lockard, D. P., Khorrami, M. R., Choudhari, M. M., Hutcheson, F. V., Brooks, T. F., and Stead, D. J., "Tandem Cylinder Noise Predictions," *13th AIAA/CEAS Aeroacoustics Conference*, 2007.